Materials Science Forum
ISSN: 1662-9752, Vol. 1130, pp 25-34
doi:10.4028/p-rNtYY7

Submitted: 2023-11-23
Revised: 2024-03-08
Accepted: 2024-03-20
Online: 2024-10-31

Influence of Different Aging Times and Temperatures on Microstructural and Mechanical Properties of EN AW-6XXX Aluminum Alloys

Chiara Soffritti[a]*, Cindy Morales[b], Annalisa Fortini[c], Mattia Merlin[d]

Department of Engineering (DE), University of Ferrara, Via Saragat 1, 44122 Ferrara, Italy

Corresponding author: [a]chiara.soffritti@unife.it, [b]mrlcdy@unife.it, [c]annalisa.fortini@unife.it, [d]mattia.merlin@unife.it

Keywords: Wrought aluminum alloys; Heat treatment; Microstructure; Mechanical properties.

Abstract. The heat-treatable EN AW-6005 and EN AW-6060 alloys are by far the most used alloys for manufacturing extruded parts for automotive, aerospace, food and healthcare industries. The strength of these alloys is usually achieved by T6 heat treatment, whose efficacy depends on the chemical composition and solubilization/aging times and temperatures. This study aims to evaluate the influence of aging parameters on the microstructural and mechanical properties of two extruded components made of the above-mentioned alloys and supplied by a healthcare company. Samples were drawn by both parts in as-received condition. Part of them was directly artificially aged at different aging times and temperatures, while the rest was subjected to tailored T6-type heat treatments. The microstructure was first analyzed by optical and scanning electron microscopy. The mechanical properties were then investigated by Brinell hardness and Vickers microhardness measurements. At last, all hardness data were compared to those obtained on specimens drawn from two other components made of the same alloys, which were heat-treated according to the parameters commonly used by the company. Based on the results, the microstructure of both components exhibited coarse grains plus lamellar and rounded intermetallic particles. Irrespective of the heat treatment route, no changes were detected in the microstructure. For each alloy, the heat treatment conditions that guarantee the best mechanical resistance were established.

Introduction

Aluminum has good extrudability, and the heat-treatable Al-Mg-Si aluminum alloys (6XXX series) are nowadays the most used alloys for manufacturing extruded parts for automotive, aerospace, food and healthcare industries [1]. Among the 6XXX series, alloys such as EN AW-6005 and EN AW-6060 cover a great share of the total extruded volume thanks to a favorable combination of properties such as high strength to weight ratio, excellent formability, good corrosion resistance and outstanding response to surface finishing procedures [2-4]. The strength of these alloys is usually achieved by precipitation hardening (or T6 heat treatment), i.e., a heat treatment that involves three main stages: (i) a first solubilization step at a high temperature; (ii) a rapid quenching to room temperature to generate a supersaturated solid solution (SSSS) of alloying elements; (iii) a final artificial aging (AA) consisting of the controlled decomposition of the SSSS to create a dispersion of sub-micrometric particles into the metal matrix [5]. During this process, the alloying elements exert, to various degrees, solution and dispersion hardening effects, with Mg and Si being the major solid-solution strengtheners [6]. In the literature, the generally accepted sequence for the formation of nano-sized particles during precipitation hardening is as follows: SSSS → clusters/GP zones → pre-β″/β″ → β′ → β, where "GP zones" stands for Guinier-Preston zones. The needle-like β″ phase is regarded as the most effective hardening phase for Al-Mg-Si aluminum alloys [7-11]. Nevertheless, it was also found that the addition of Cu to the alloys of 6XXX group modifies the above-mentioned sequence as: SSSS → clusters/GP zones → β″, L, C, QP, QC → β′, Q′ → Q. Hence, the precipitation of more metastable phases accompanying β″ is claimed to strongly influence the strength of EN AW-6005 and EN AW-6060 aluminum alloys [12].
In general, the efficacy of precipitation hardening in improving the performance of Al-Mg-Si aluminum alloys depends on several factors such as the chemical composition of the alloy and

solubilization/aging time and temperature [6,13-17]. G. Mrówka-Nowotnik et al. [13] evaluated the influence of different solubilization temperatures (from 510 °C to 580 °C) and cooling conditions (quench in oil, water, air and slow furnace cooling) on the microstructure and mechanical properties of commercial 6005 and 6082 wrought alloys. They found that the hardness of the 6082 alloy increased with rising quench severity and, to a minor extent, solubilization temperature; conversely, the hardness and aging kinetics of the 6005 alloy were not affected by the solubilization parameters. In [14], an experimental investigation on artificial aging of 6061-T6 alloy was conducted by varying the aging temperature between 175 °C and 420 °C, and the aging time from 30 min to 10 hours. The authors demonstrated that the optimum aging could be obtained at temperatures from 175 °C to 195 °C for times from 2 to 6 hours; especially, the maximum strength was referred to the samples aged at 185 °C for 6 hours. Similar results were reported by Polat et al. in [6]. For the same aluminum alloy, it was suggested that the best compromise between hardness, yield and tensile strength, and elongation could be attained with artificial aging at 180 °C for times between 5 and 40 hours. Ding et al. [15] highlighted that the amount of sub-micrometric precipitates in the microstructure of aged 6005A extrusions was maximum at 175 °C. In addition, aging times from 4 to 8 hours enabled to reach yield and tensile strength in longitudinal direction of more than 270 and 300 MPa, respectively. Different artificial aging at under-, peak- and over-aged temperatures were performed by Siddiqui et al. [16] with the aim of evaluating their influence on the mechanical properties of 6063 alloy. Based on the results, aging at 175 °C for times from 8 and 10 hours was able to guarantee the greatest mechanical resistance, but the best fatigue fracture behavior was registered for samples aged at 200 °C for 6 hours. In under- and peak-aged conditions (i.e., for aging temperatures ≤ 200 °C and times of at least 8 hours), the strengthening effect was a result of two main mechanisms: (a) the impedance of dislocation motion and (b) the high mobility of vacancies playing a pivotal role in the generation of GP zones. In over-aged conditions (i.e., for aging temperatures > 200 °C and times longer than 8 hours), the coalescence of nano-sized particles into large precipitates occurred with a consequent decrease in their capability to hinder the movement of dislocations. This phenomenon led, in turn, to a worsening of the mechanical properties of the alloy. Concerning the 6022 alloy, peak-aged conditions were achieved at aging temperatures higher than 200 °C and for aging times less than 2 hours [17].

In industrial practice, extruded components are unavoidably subjected to short- or long-term storage before artificial aging. During this time, natural pre-aging (NA) at room temperature would occur, producing clusters or co-clusters of dissolved alloying elements (mostly Mg and Si) [18]. In the literature, the effects of natural pre-aging on the hardening response of the material during the subsequent artificial aging can be stated as either positive or negative ones in relation to the alloy chemistry: when the total amount of Mg + Si < 1 wt% NA is positive, the opposite when Mg + Si ≥ 1 wt% [19,20]. In the first case, it was reported that the AA of natural pre-aged lean alloys slowly dissolved the vacancy-free co-clusters favoring the hardness and strength increase at the aging temperatures [18,21-23]. In the second case, some studies assigned the adverse influence of NA on AA to the depletion of supersaturated solutes in metal matrix caused by the formation of durable NA clusters, being unfavorable nucleation sites for precipitation of β″ phase during artificial aging [24,25]. Other research further demonstrated that the same clusters could annihilate or trap the quenched-in vacancies, thus retarding the precipitation process by slowing down solution diffusion [26]. Nevertheless, Martinsen et al. [27] assessed that in 6005 and 6060 alloys the negative NA effect may be reversed upon long-term storage (higher than the typical industrial storage time of 4 hours), but also at very early stages of natural pre-aging (30 min and below).

In this framework, this study aims to evaluate the influence of aging parameters on the microstructural and mechanical properties of two industrial components supplied by a healthcare company and made of EN AW-6005 and EN AW-6060 aluminum alloys. A number of samples were drawn by both parts in as-received condition. Part of the specimens was directly artificially aged at different combinations of aging time and temperature, while the rest was subjected to tailored T6-type heat treatments. The microstructure of as-received and heat-treated samples was first investigated by optical microscopy and scanning electron microscopy equipped with energy

dispersive spectroscopy. The mechanical properties were then determined by hardness measurements. Finally, all hardness data were compared to those obtained on other two components made of the same aluminum alloys, which were heat-treated according to the parameters commonly used by the company.

Materials and Methods

Two extruded components (labeled as C1 and C2) made of EN AW-6005 and EN AW-6060 aluminum alloys, respectively, were provided by FERNO S.r.l., a commercial company operating in the healthcare industry. Details of the nominal chemical composition of the alloys are reported in Table 1.

Table 1 Nominal chemical composition [wt%] of the alloys employed in this study.

	Si	Mg	Mn	Cu	Cr	Zn	Ti	Fe	Al
EN AW-6005	0.60-0.90	0.40-0.60	≤ 0.10	≤ 0.10	≤ 0.10	≤ 0.10	≤ 0.10	≤ 0.35	Balance
EN AW-6060	0.30-0.60	0.35-0.50	0.10	≤ 0.10	≤ 0.05	≤ 0.15	≤ 0.10	0.10-0.30	Balance

In as-received condition, both parts were in T4 state, i.e., solution heat treated and naturally aged at room temperature until reaching a substantially stable condition. From each component, samples were drawn in longitudinal direction (parallel to the metal surface) and cross-direction (perpendicular to the metal surface) by a TR80 EVOLUTION (Remet, Bologna, Italy) cutting machine. Three specimens per section were mounted in resin, polished and analyzed by a Leica DMi8 A optical microscope (Leica, Wetzlar, Germany) under polarized light exposure. The microstructural investigations were carried out after electrolytic etching in Barker's reagent (4-5 ml HBF_4 (48 %), 200 ml distilled water) by applying a direct current of 15 V for 1 min through a Polectrol (Struers, Copenaghen, Denmark) power supply. For each aluminum alloy, nine composite micrographs were acquired in cross-section to calculate the average grain size. Each composite micrograph consisted of nine images taken at a magnification of 500x, which guaranteed the investigation of an area sufficiently representative of the entire sample. In this area, a minimum of 300 grains were processed following the intercept method described in the UNI EN ISO 643:2020 standard. An in-depth analysis of the microstructure was also conducted by a Zeiss EVO MA 15 (Zeiss, Oberkochen, Germany) scanning electron microscope equipped with an Oxford X-Max 50 (Oxford Instruments, Abingdon-on-Thames, UK) microprobe for energy-dispersive spectroscopy (SEM/EDS). The SEM micrographs were recorded in secondary electron imaging (SEI-SEM) and back-scattered electron (BSE-SEM) mode.
For C1 component, the mean Brinell hardness was evaluated in agreement with the UNI EN ISO 6506-1:2015 standard by a ERNST AT-130D (CISAM-ERNST S.r.l., Induno Olona, Italy) tester, using a tungsten carbide ball 2.5 mm in diameter and a 62.5 kg_f load for 15 s. Each hardness value was an average of five measurements. No Brinell hardness measurements were collected for the C2 due to geometric constraints. A Future-Tech FM-110 (Future-Tech Corp., Kawasaki, Japan) microindenter was also employed for determining the mean Vickers microhardness (HV0.1) of both components under a 100 g_f load for 15 s and according to the UNI EN ISO 6507-1:2018 standard. The mean value was calculated as an average of ten indentations.

Table 2 Details of direct aging parameters employed in this study.

C1 (EN AW-6005)	C2 (EN AW-6060)
170 °C / 4, 6, 8, 10 h	170 °C / 4, 6, 8, 10 h
180 °C / 4, 6, 8, 10 h	180 °C / 4, 6, 8, 10 h
185 °C / 4, 6, 8, 10 h	185 °C / 4, 6, 8, 10, 15, 20 h
190 °C / 4, 6, 8, 10 h	190 °C / 4, 6, 8, 10 h

Two different heat treatment routes were then adopted. Part of the samples was directly artificially aged (DA) at different temperatures (between 170 °C and 190 °C) and for different aging times (from 4 to 20 h) in a Lenton LTF 12 (Lenton Furnaces & Ovens, Hope, UK) tube furnace. The rest of the specimens was subjected to tailored T6-type heat treatments consisting of: (i) a solubilization step at 540 °C for 1 h in a REMET mod. E-79N (Remet, Italy) muffle furnace; (ii) water quenching to room temperature; (iii) final artificial aging at 180 °C for 4, 6, 8 and 10 h in the same tube furnace. It should be pointed out that before AA the quenched samples were stored at -20 °C to avoid natural pre-aging. For the aluminum alloys under investigation, all heat treatment routes were established in agreement with [6,13-17]. Details of direct aging parameters employed in this study are summarized in Table 2, while a scheme of T6-type heat treatments is shown in Fig. 1.

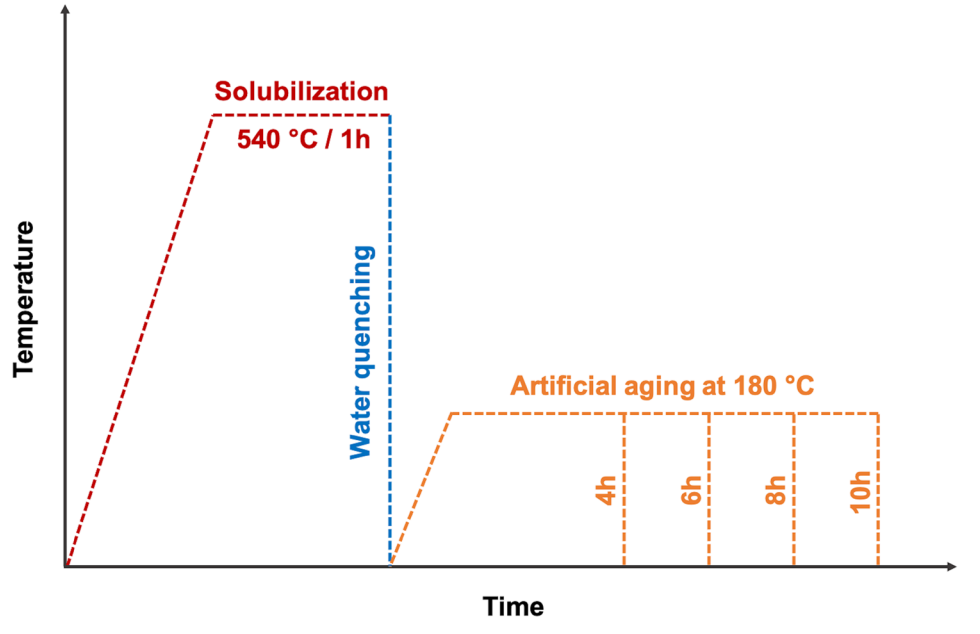

Fig. 1 Scheme of T6-type heat treatments.

After heat treatment, the microstructure and mechanical properties of all samples were evaluated by the already described procedure. Finally, all hardness data were compared to those obtained on specimens drawn from two other components made of the same aluminum alloys, which were heat-treated according to the parameters commonly used by the company and subsequently characterized by the above-mentioned instrumentations. These latter heat treatment parameters are confidential.

Results and Discussion

The representative optical micrographs in Fig. 2 depict the microstructure of C1 and C2 components observed in the longitudinal section and cross-section, respectively. Both micrographs were collected on samples in as-received condition and after electrolytic etching in Barker's reagent.

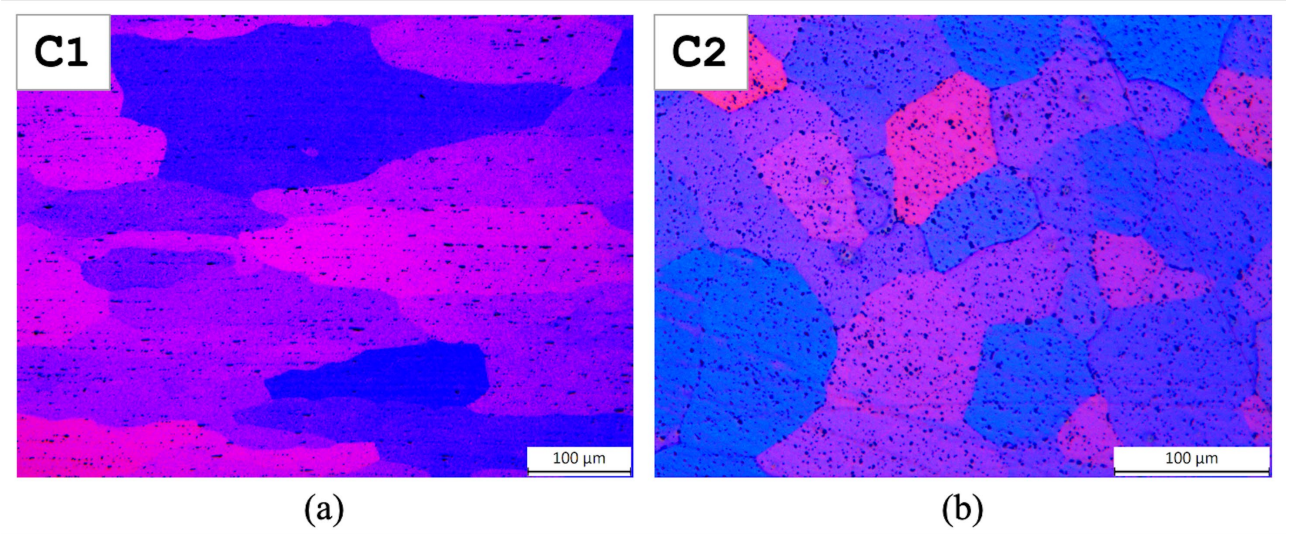

Fig. 2 Representative optical micrographs of the microstructure of C1 and C2 components observed in (a) longitudinal section and (b) cross-section. Both images were collected on samples in as-received condition and after electrolytic etching in Barker's reagent.

In the T4 state, the microstructure of the two extruded parts consisted of coarse equiaxed grains with a great number of intermetallic particles uniformly distributed in the metal matrix (Fig. 2a and b). In cross-section, the calculated average grain size of C1 component (corresponding to EN AW-6005 alloy) was 83 µm, whereas that of the C2 (corresponding to EN AW-6060 alloy) was 87 µm. In the longitudinal section, grains and inclusions were arranged parallel to plastic deformation (Fig. 2a), thus generating a fibrous microstructure.

Based on the SEM/EDS observations, the intermetallic particles (light contrast areas in the BSE-SEM micrograph of Fig. 3) displayed lamellar and rounded morphology. The semi-quantitative EDS analysis of lamellar inclusions indicated the presence of aluminum, silicon, iron, manganese and chromium (site 1 in Fig. 3b), with a (Fe + Mn + Cr)/Si ratio, expressed as atomic percentage [at%], around 1.0. As a result, these particles could be ascribed to the β-Al(FeMnCr)Si phase [13]. Concerning rounded particles, the same elements were detected (site 2 in Fig. 3b), but with a (Fe + Mn + Cr)/Si ratio of about 1.5; hence, these intermetallics could be determined as the α-Al(FeMnCr)Si phase [28]. All EDS results are consistent with previously reported data for extruded Al-Mg-Si alloys [29,30].

Irrespective of the heat treatment route, the microstructure and average grain size of heat-treated samples were similar to those of as-received specimens. As already detailed in the Introduction section, the main outcome of aging process is the strengthening of alloys due to the precipitation of sub-micrometric particles in the metal matrix [5]. The density of these precipitates is strongly affected by the heat treatment parameters, with the aging kinetic being controlled by the diffusion of the solute atoms [31]. With reference to the aging sequence reported in the same section, the GP-I zones with a size in the range of 1–3 nm are the earliest particles able to produce a distinct contrast for identification by the more recent transmission electron microscopy techniques [32]. It should be highlighted that the needle-like β″ phase has been considered as the most developed GP-I zones [21]. Accordingly, no microstructural changes could be recognized in heat-treated samples due to the limited resolution of the microscopy instrumentations employed in this study.

Element	at%
Mg K	0.51
Al K	88.39
Si K	4.21
Cr K	0.22
Mn K	0.73
Fe K	5.56
Cu K	0.38
Totals	100.00

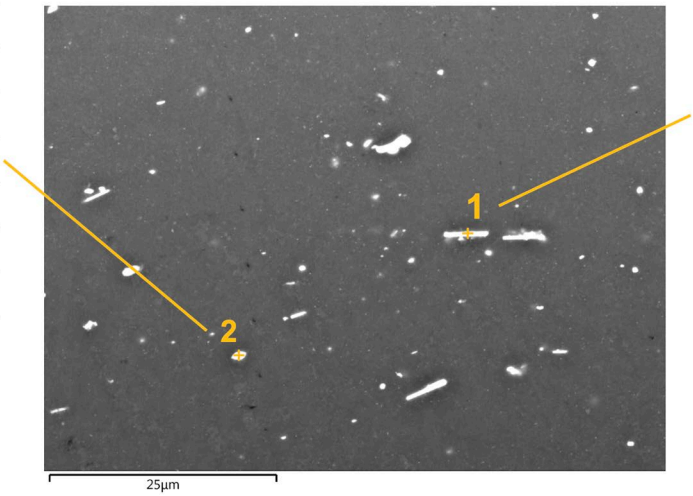

Element	at%
Mg K	0.62
Al K	85.07
Si K	7.34
Cr K	0.16
Mn K	0.23
Fe K	6.25
Cu K	0.33
Totals	100.00

Fig. 3 BSE-SEM micrograph of the microstructure of C1 component observed in cross-section and semi-quantitative EDS results (expressed as atomic percentage [at%]) of lamellar and rounded particles in the same microstructure (sites 1 and 2, respectively).

Concerning the mechanical properties of the two components in cross-section and in as-received condition, the C1 showed a mean HB10 of 72 ± 2 and a mean HV0.1 of 72.8 ± 2.5, whereas the C2 exhibited a mean Vickers microhardness of 42.9 ± 2.0.

The mean values ± standard deviations of Brinell hardness of C1 component measured in cross-section and after the two different heat treatment routes are shown in Fig. 4. First of all, it should be noted that the mean Brinell hardness of most samples subjected to T6-type heat treatments (Fig. 4b) was higher than that of directly aged specimens (Fig. 4a). Since the extruded part was in T4 state before heat treatments, this could suggest the occurrence of a negative natural pre-aging effect, which was partially withdrawn by the subsequent precipitation hardening. Considering the nominal chemical composition of EN AW-6005 alloy collected in Table 1, this is in agreement with the literature data for natural pre-aged 6xxx alloys containing a total amount of Mg + Si ≥ 1 wt% [19,20]. After direct aging, the mean HB10 increased with increasing aging time and temperature (Fig. 4a), with the highest mean values being obtained for aging temperatures between 180 °C and 190 °C and for aging times of 8-10 h (blue dotted lines in the same figure). When the same alloy was solubilized at 540 °C for 1 h, water quenched to room temperature and artificial aged at 180 °C for 10 h, the mean Brinell hardness was maximum and equal to 114 ± 7 (Fig. 4b). A comparison between the mean HB10 registered under these latter heat treatment conditions and the mean Brinell hardness of the alloy heat-treated according to the company parameters (purple bar in Fig. 4b) enable to estimate an increase in mechanical resistance of about 12 %.

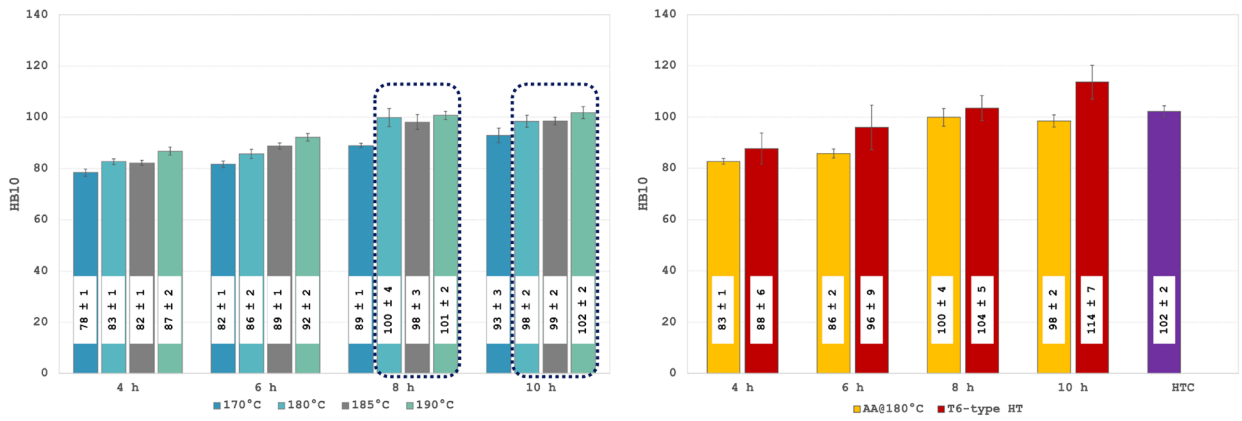

Fig. 4 Mean values ± standard deviations of Brinell hardness of C1 component measured in cross-section and after: (a) direct aging at the different combinations of aging time and temperature; (b) T6-type heat treatments. The blue dotted lines in (a) enclose the direct aging conditions displaying the highest mean Brinell hardness. In (b), the HB10 of samples directly aged at 180 °C for 4, 6, 8 and 10 h and that of the same component heat-treated by the company were also included. (HT = heat treatment; HTC = heat treatment performed by the company)

Figure 5 depicts the mean values ± standard deviations of Vickers microhardness of C2 component measured in cross-section and after the two different heat treatment routes. As for the C1 extruded part, the mean Vickers microhardness of several samples subjected to T6-type heat treatments (Fig. 5b) was slightly higher than that of directly aged specimens (Fig. 5a). Accordingly, it was supposed that also the EN AW-6060 alloy experienced a negative natural pre-aging effect, albeit to a minor extent. In this case, the results are partially in agreement with the literature data for natural pre-aged 6xxx alloys containing a total amount of Mg + Si < 1 wt% [19,20]. Concerning direct aging, once the aging time is fixed, no specific trends of HV0.1 can be defined for the different aging temperatures (Fig. 5a). Besides, the highest mean values of Vickers microhardness were obtained with DA at 170 °C and 190 °C for 8 h, and at 170 °C for 10 h (blue dotted lines in the same figure). Direct aging at 185 °C for 15 and 20 h led to mean HV0.1 of 77.5 ± 2.1 and 79.7 ± 1.8, respectively. These values are similar to the highest ones; nevertheless, the achieved mechanical properties do not justify the adoption of such time and energy-consuming heat treatments. When the EN AW-6060 alloy underwent a T6-type heat treatment comprising artificial aging at 180 °C for 10 h, the mean HV0.1 was maximum and equal to 83.0 ± 1.5 (Fig. 5b). A comparison between the mean Vickers microhardness measured under these latter heat treatment conditions and the mean HV0.1 of the alloy heat-treated according to the company parameters (purple bar in Fig. 5b) enable to assess, once again, an increase in the mechanical resistance of about 12 %.

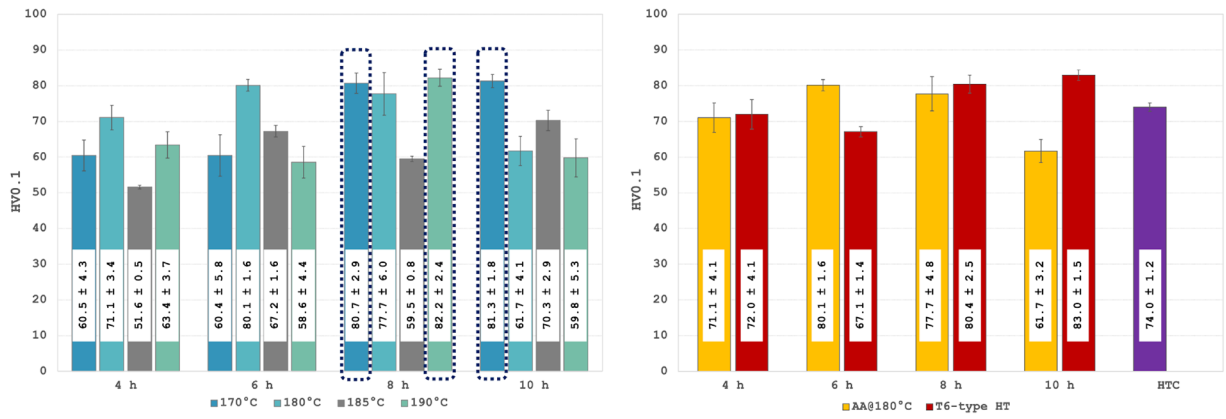

(a) (b)

Fig. 5 Mean values ± standard deviations of Vickers microhardness of C2 component measured in cross-section and after: (a) direct aging at the different combinations of aging time and temperature; (b) T6-type heat treatments. The blue dotted lines in (a) enclose the direct aging conditions displaying the highest mean Vickers microhardness. In (b), the HV0.1 of samples directly aged at 180 °C for 4, 6, 8 and 10 h and that of the same component heat-treated by the company were also included. (HT = heat treatment; HTC = heat treatment performed by the company)

Conclusions

This study investigates the effects of different aging times and temperatures on the microstructure and mechanical properties of two extruded components for healthcare industry, which were made of EN AW-6005 and EN AW-6060 aluminum alloys. Based on the results, the following conclusions can be drawn:

- The microstructure of both components exhibited coarse equiaxed grains (with an average grain size between 83 and 87 μm in cross-section) plus lamellar and rounded intermetallic particles, which could be ascribed to the β-Al(FeMnCr)Si and α-Al(FeMnCr)Si phases.
- Irrespective of the heat treatment route, no changes were detected in the microstructure and average grain size.
- For the EN AW-6005 alloy, the highest mean Brinell hardness was obtained after direct aging between 180 °C and 190 °C for 8-10 h and after artificial aging at 180 °C for 10 h during T6-type heat treatment.
- For the EN AW-6060 alloy, the highest mean Vickers microhardness was obtained after direct aging at 170 °C and 190 °C for 8 h, and at 170 °C for 10 h. The mean HV0.1 was then maximum after T6-type heat treatment comprising AA at 180 °C for 10 h.
- Finally, all the above-mentioned heat treatments favored an increase in the mechanical resistance up to about 12 % with respect to that of the alloys heat-treated according to the company parameters.

Acknowledgments

The authors wish to acknowledge Eng. Vittorio Ghelli for his valuable contribution to the experimental part of the present investigation, and FERNO S.r.l. (Pieve di Cento, BO, Italy) for the financial support and the supply of the material examined.

References

[1] K. Anderson, J. Weritz, J.G Kaufman, Properties and Selection of Aluminum Alloys, Vol. 2B, ASM International, Materials Park, Ohio, USA, 2019.

[2] J. Røyset, U. Tundal, C. Espezel, O. Reiso, Al-Mg-Si billets with high extrudability – state of the art and beyond, Mater. Today Proc. 10 (2019) 185-192.

[3] Y. Birol, Precipitation during homogenization cooling in AlMgSi alloys, T. Nonferr. Metal. Soc. 23 (2013) 1875-1881.

[4] O. Reiso, Proc. 9th International Conference on Aluminium Alloys (ICAA9) Aug. 2-5 2004, Brisbane, Australia, Eds. J.F. Nie, A.J. Morton and B.C. Muddle, Vol. 1, pp. 32–46.

[5] R. Mimica, Hardness versus time dependency during artificial ageing of AlMgSi0.5 aluminium alloy, Mater. Sci. L51 (2015) 261-268.

[6] A. Polat, M. Avsar, F. Ozturk, Effects of the artificial-aging temperature and time on the mechanical properties and springback behavior of AA6061, Mater. Tehnol. 49(2015)487-493.

[7] J. Buha, R.N. Lumley, A.G. Crosky, K. Hono, Secondary precipitation in an Al-Mg-Si-Cu alloy, Acta Mater. 55 (2007) 3015-3024.

[8] C.D. Marioara, H. Nordmark, S.J. Andersen, R. Holmestad, Post-β″ phases and their influence on microstructure and hardness in 6xxx Al-Mg-Si alloys, J. Mater. Sci. 41 (2006) 471-478.

[9] S. Pogatscher, H. Antrekowitsch, H. Leitner, T. Ebner, P.J. Uggowitzer, Mechanisms controlling the artificial aging of Al–Mg–Si alloys, Acta Mater. 59 (2011) 3352-3363.

[10] J.H. Chen, E. Costan, M.A. van Huis, Q. Xu, H.W. Zandbergen, Atomic pillar-based nanoprecipitates strengthen AlMgSi alloys, Science 312 (2006) 416-419.

[11] C. Ravi, C. Wolverton, First-principles study of crystal structure and stability of Al–Mg–Si–(Cu) precipitates, Acta Mater. 52 (2004) 4213-4227.

[12] M. Torsæter, W. Lefebvre, C.D. Marioara, S.J. Andersen, J.C. Walmsley, R. Holmestad, Study of intergrown L and Q′ precipitates in Al–Mg–Si–Cu alloys, Scr. Mater. 64 (2011) 817-820.

[13] G. Mrówka-Nowotnik, J. Sieniawski, Influence of heat treatment on the microstructure and mechanical properties of 6005 and 6082 aluminium alloys, J. Mat. Process. Tech. 162–163 (2005) 367-372.

[14] C.F. Tan, M.R. Said, Effect of hardness test on precipitation hardening aluminium alloy 6061-T6, J. Mater. Process. Tech. 36 (2009) 276-286.

[15] X. Ding, J. Sun, J. Ying, W. Zhang, J. Ma, L. Wang, Influences of aging temperature and time on microstructure and mechanical properties of 6005A aluminum alloy extrusions, T. Nonferr. Metal. Soc. 22 (2012) s14-s20.

[16] R.A. Siddiqui, H.A. Abdullah, K.R. Al-Belushi, Influence of aging parameters on the mechanical properties of 6063 aluminium alloy, J. Mater. Process. Tech. 102 (2000) 234-240.

[17] J.J. Gracio, F. Barlat, E.F. Rauch, P.T. Jones, V.F. Neto, A.B. Lopes, Artificial aging and shear deformation behaviour of 6022 aluminium alloy, Int. J. Plasticity 20 (2004) 427-445.

[18] U. Stamenković, S. Ivanov, I. Marković, S. Mladenović, D. Manasijević, L. Balanović, The influence of natural aging and pre-aging on the mechanical, physical and microstructural properties of the EN AW-6060 aluminum alloy, Machines. Technologies. Materials. 13 (2019) 187-189.

[19] M. Torsæter, H.S. Hasting, W. Lefebvre, C.D. Marioara, J.C. Walmsley, S.J. Andersen, R. Holmestad, The influence of composition and natural aging on clustering during preaging in Al–Mg–Si alloys, J. Appl. Phys. 108 (2010) 073527.

[20] G.H. Tao, C.H. Liu, J.H. Chen, Y.X. Lai, P.P. Ma, L.M. Liu, The influence of Mg/Si ratio on the negative natural aging effect in Al–Mg–Si–Cu alloys, Mat. Sci. Eng. A-Struct. 642 (2015) 241-248.

[21] S. Pogatscher, H. Antrekowitsch, T. Ebner, P.J. Uggowitzer, The role of co-clusters in the artificial aging of AA6061 and AA6060 in: C.E. Suarez (Ed.), Light Metals, Springer, Cham., 2012.

[22] F. De Geuser, W. Lefebvre, D. Blavette, 3D atom probe study of solute atoms clustering during natural ageing and pre-ageing of an Al-Mg-Si alloy, Philos. Mag. Lett. 86 (2006) 227-234.

[23] C.S.T. Chang, I. Wieler, N. Wanderka, J. Banhart, Positive effect of natural pre-ageing on precipitation hardening in Al–0.44 at% Mg–0.38 at% Si alloy, Ultramicroscopy 109 (2009) 585-592.

[24] K. Yamada, T. Sato, A. Kamio, Effects of quenching conditions on two-step aging behavior of Al-Mg-Si alloys, Mater. Sci. Forum 331-337 (2000) 669-674.

[25] J. Røyset, T. Stene, J.A. Sæter, O. Reiso, The effect of intermediate storage temperature and time on the age hardening response of Al-Mg-Si alloys, Mater. Sci. Forum 519-521 (2006) 239-244.

[26] J. Banhart, C.S.T. Chang, Z. Liang, N. Wanderka, M.D.H. Lay, A.J. Hill, Natural aging in Al-Mg-Si alloys–a process of unexpected complexity, Adv. Eng. Mater. 12 (2010) 559-571.

[27] F.A. Martinsen, F.J.H. Ehlers, M. Torsæter, R. Holmestad, Reversal of the negative natural aging effect in Al–Mg–Si alloys, Acta Mater. 60 (2012) 6091-6101.

[28] M.S. Silva, C. Barbosa, O. Acselrad, L.C. Pereira, Effect of chemical composition variation on microstructure and mechanical properties of a 6060 aluminum alloy, J. Mater. Eng. Perform. 13 (2004) 129-134.

[29] S. Yuan, L. Chen, J. Tang, G. Zhao, C. Zhang, J. Yu, Correlation between homogenization treatment and subsequent hot extrusion of Al–Mg–Si alloy, J. Mater. Sci. 54 (2019) 9843-9856.

[30] Y. Birol, Optimization of homogenization for a low alloyed AlMgSi alloy, Mater. Charact. 80 (2013) 69-75.

[31] S. Pogatscher, H. Antrekowitsch, H. Leitner, A.S. Sologubenko, P.J. Uggowitzer, Influence of the thermal route on the peak-aged microstructures in an Al–Mg–Si aluminum alloy, Scripta Mater. 68 (2013) 158-161.

[32] E. Thronsen, J. Frafjord, J. Friis, C.D. Marioara, S. Wenner, S.J. Andersen, R. Holmestad, Studying GPI zones in Al-Zn-Mg alloys by 4D-STEM, Mater. Charact. 185 (2022) 111675.